AIAA-81-1675
Lift Enhancing
Surfaces on Several
Advanced V/STOL Fighter/Attack
Aircraft Concepts

D. A. Durston and S. C. Smith
NASA Ames Research Center
Moffett Field, CA

AIAA Aircraft Systems
and Technology Conference

August 11-13, 1981/Dayton, Ohio

LIFT-ENHANCING SURFACES ON SEVERAL ADVANCED V/STOL FIGHTER/ATTACK AIRCRAFT CONCEPTS

Donald A. Durston* and Stephen C. Smith*
Ames Research Center, NASA, Moffett Field, California

Abstract

An analysis of the relative influences of forward lift-enhancing surfaces on the overall lift and drag characteristics of three wind-tunnel models representative of V/STOL fighter/attack aircraft is presented. Two of the models are canard-wing configurations and one has a wing leading-edge extension (LEX) as the forward lifting surface. Data are taken from wind-tunnel tests of each model covering Mach numbers from 0.4 to 1.4. Overall lift and drag characteristics of these models and the generally favorable interactions of the forward surfaces with the wings are highlighted. Results indicate that larger LEX's and canards generally give greater lift and drag improvements than ones that are smaller relative to the wings.

Nomenclature

ALT = alternate LEX, VATOL configuration (has 1/2 the planform area of the standard LEX)

B.L. = buttock line, spanwise distance from model centerline

C_D = drag coefficient, drag/q S_{REF}

C_L = lift coefficient, lift/q S_{REF}

C_{L_α} = lift curve slope, dC_L/d_α

C_R = root chord

C_T = tip chord

f_L = lift-enhancing surface lift efficiency factor

f_o = lift-enhancing surface drag efficiency factor

F.S. = fuselage station

LEX = leading-edge extension

L/D = lift-to-drag ratio

M = free-stream Mach number

MAC = mean aerodynamic chord

q = free-stream dynamic pressure

R_a = S_a/S_{REF}

S_a = exposed surface area of LEX or canard

S_{REF} = model reference area; equal to total planform area, unless otherwise stated

STD = standard LEX, VATOL configuration

W.L. = waterline, vertical distance from model centerline

α = angle of attack

Δ = increment between zero and nonzero canard deflection

δ_{CANARD} = canard deflection angle, positive LE up

Subscripts

a = additional surface, or lift-enhancing surface

TOT = total; that is, with additional surface

Introduction

V/STOL fighter aircraft offer potentially significant improvements in operational flexibility for Navy and Air Force missions. Such aircraft with supersonic capability and good transonic maneuverability can be available in the mid- to late 1990's. To help establish a useful aerodynamic data base for this class of aircraft, Ames Research Center is currently conducting a number of programs to develop the aerodynamic technology for future V/STOL aircraft. One of these programs, jointly sponsored by Ames and the David Taylor Naval Ship Research and Development Center (DTNSRDC), addresses the aerodynamic and airframe-propulsion integration technology requirements projected for V/STOL fighter/attack aircraft in the 1990's.

This program was conducted in two phases. In Phase I, V/STOL fighter/attack aircraft concepts were defined and their aerodynamic uncertainties identified. Then prediction methods were applied to provide estimates of the aircraft aerodynamics. Phase II consisted of wind-tunnel tests of these concepts to investigate the uncertainties and to assess the prediction methods. General Dynamics, Grumman, Northrop, and Vought participated in Phase I under contract to Ames Research Center.[1-6] General Dynamics and Northrop continued with Phase II. (At the time of the publication of this paper, Phase II was nearly complete.) References 7 through 11 cover some of the results of the Phase II efforts.

The wind-tunnel models developed in the program are representative of highly maneuverable V/STOL fighter aircraft. To achieve this maneuverability, forward lifting surfaces, such as canards, strakes, and leading-edge extensions (LEX's), are used to enhance the flow over the wings. Through extensive generic research, these surfaces have been found to contribute to higher lift with lower drag than configurations without them. The work of Luckring[12] and Re and Capone[13] quantified the advantages of strakes and canards at low subsonic (M = 0.3) through transonic (M = 1.2) speeds on generic research models. Their data show increases in lift and decreases in drag as a result of the flow from the strake or canard acting on the wing.

This paper focuses on an extension of this generic research to practical fighter configurations at speeds from subsonic through supersonic and at flow angles to approximately 25°. In particular, the overall lift and drag benefits of the forward lift-enhancing surfaces (i.e., leading-edge extensions and canards) are presented for the models developed in the aforementioned Ames Research Center program. The objective of the paper is to show the effects of the aerodynamic interaction between the foreard lifting surfaces and the wings on these V/STOL fighter configurations.

V/STOL Fighter/Attack Aircraft Configurations

The configurations under investigation are shown in Fig. 1. On the left side of the figure is an artist's rendering of Northrop's VATOL (vertical attitude takeoff and landing) concept[5] and a photograph of the representative model in the wind tunnel. As the name implies, this is a tail-sitter-type V/STOL aircraft that uses the rear nozzles for lift without large exhaust nozzle deflections. The forward lift-enhancing surface is a LEX, which delays wing stall and increases maximum lift through vortex interaction with the wing upper surface flow field. Reference 14 presents water-tunnel studies that illustrate the vortical flow fields from LEX's on various configurations. The center of Fig. 1 shows the General Dynamics HATOL (horizontal attitude takeoff and landing) concept.[2] A pair of jet diffuser ejectors located between the engine nacelles on either side of the fuselage provides the propulsive lift for takeoff and landing. The primary lift-enhancing surface during wing-supported flight is a close-coupled canard. In addition, a strake inboard of the engine nacelles works in conjunction with the inboard wing to provide further lift enhancements when the ejectors are closed. The third concept shown in the figure is a Northrop HATOL design,[4] which uses a RALS (remote augmenta-tion lift system) as a forward lift system with twin ADEN's (augmented deflector exhaust nozzles) in the rear. An inlet-mounted close-coupled canard is also used in this concept as the lift-enhancing surface. For the purposes of this paper, these three models will be referred to hereinafter by their type of propulsive lift system: "VATOL" (which implies no additional primary propulsive lift system) for the Northrop VATOL concept, "Ejector" for the General Dynamics HATOL, and "RALS" for the Northrop HATOL.

Three-view drawings of these wind-tunnel models are shown in Figs. 2-4. Basic dimensional data are provided in Tables 1-3. These versatile models have interchangeable and removable parts that allow for testing of a wide range of configuration options: various combinations of wing leading- and trailing-edge flap deflections, canard deflections (RALS and Ejector models), different canard longitudinal locations (Ejector), alternative LEX size (VATOL), and component buildup. Since the paper deals with the interactions between the wind and the forward surfaces of each configuration, emphasis will be on the effects of variations of these forward surfaces. Data presented in this paper are from tests in the 11-Foot Transonic Wind Tunnel at Ames Research Center. Mach numbers of 0.6, 0.9, and 1.2 at a constant unit Reynolds number of 9.84×10^6/m (3.0×10^6/ft) are covered. All data are presented untrimmed, and no pitching moment effects are discussed.

Redefinition of Reference Area

The reference area for the aerodynamic coefficients of these models is usually defined as the planform area of the wing with its leading and trailing edges extended to the fuselage centerline. This has long been the industry "standard," and is fully acceptable for models in which most of the
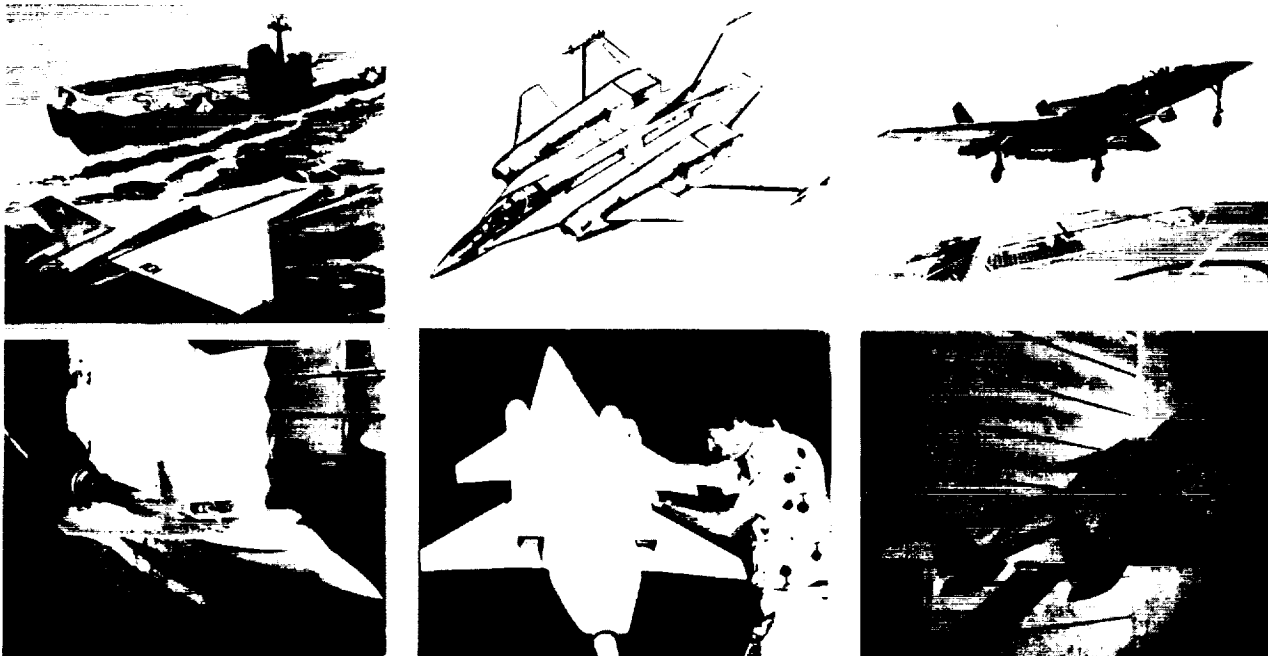

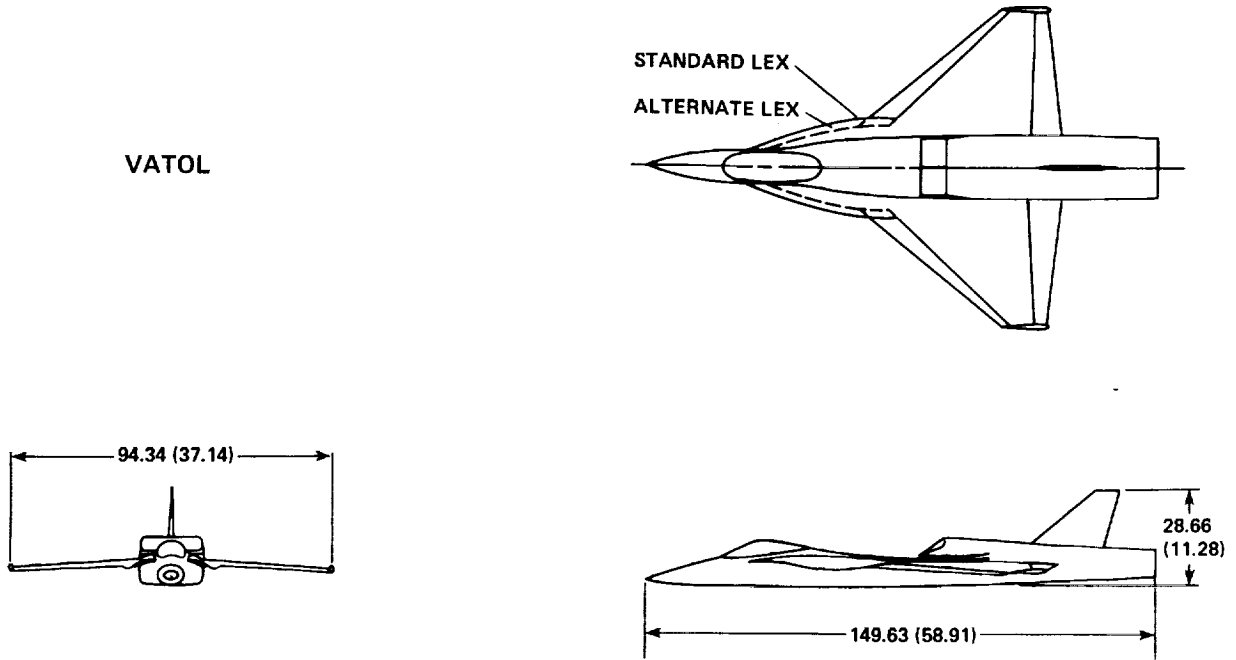Fig. 1 Artist's views and photographs of V/STOL fighter configurations.

VATOL

STANDARD LEX

ALTERNATE LEX

94.34 (37.14)

28.66 (11.28)

149.63 (58.91)

Fig. 2 Northrop VATOL configuration.

Table 1 Geometry of VATOL configuration

Property	Wing	Vertical tail
Airfoil		
Root	NACA 65A204	NACA 65A004
Tip	NACA 65A204	NACA 65A004
MAC, m (in.)	0.516 (20.33)	0.155 (6.12)
Aspect ratio	2.12	1.10
Taper ratio	0.18	0.34
Root chord, m (in.)	0.754 (29.68)	0.215 (8.46)
Tip chord, m (in.)	0.136 (5.34)	0.072 (2.85)
Span, m (in.)	0.943 (37.14)	0.158 (6.22)
Dihedral, deg	-3	---
Incidence, deg	-0	---
Twist (positive LE up at tip), deg	-6	0
Hinge line		
B.L., m (in.)	---	0
F.S., m (in.) (coincident with 0.25 MAC)	---	1.273 (50.11)
W.L., m (in.)	---	0.054 (2.12)
Hinge-line sweep, deg	---	2.5
Leading-edge sweep, deg	50	50
Exposed area, m^2 (ft^2)	0.294 (3.16)	0.023 (0.244)

Wing to centerline ref. area: 0.419 m^2 (4.51 ft^2)
Total planform ref. area: 0.545 m^2 (5.87 ft^2)
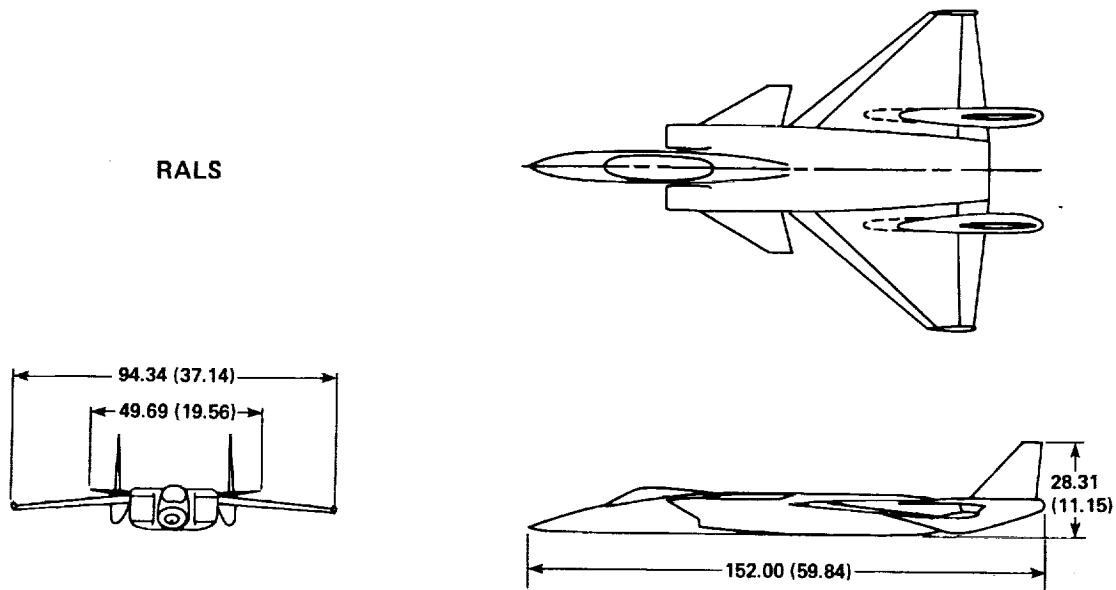Body length: 1.50 m (58.91 in.)

RALS

94.34 (37.14)

49.69 (19.56)

28.31 (11.15)

152.00 (59.84)

Fig. 3 Northrop RALS configuration.

Table 2 Geometry of RALS configuration

Property	Wing	Horizontal canard	Vertical tail
Airfoil			
Root	NACA 65A204	NACA 65A004	NACA 65A004
Tip	NACA 65A204	NACA 65A004	NACA 65A004
MAC, m (in.)	0.516 (20.33)	0.176 (6.91)	0.141 (5.56)
Aspect ratio	2.12	0.77[a]	1.31[a]
Taper ratio	0.18	0.27	0.31
Root chord, m (in.)	0.754 (29.68)	0.248 (9.79)	0.198 (7.79)
Tip chord, m (in.)	0.136 (5.34)	0.068 (2.66)	0.060 (2.38)
Span, m (in.)	0.943 (37.14)	0.122 (4.79)[a]	0.169 (6.65)
Dihedral, deg	-3	5	---
Incidence, deg	-0	---	---
Twist (positive LE up at tip), deg	-6	0	0
Hinge line			
B.L., m (in.)	---	0.128 (5.05)	0.163 (6.42)
F.S., m (in.) (coincident with 0.25 MAC)	---	0.654 (25.75)	1.42 (55.82)
W.L., m (in.)	---	0.053 (2.08)	0.061 (2.40)
Hinge-line sweep, deg	–	0	0
Leading-edge sweep, deg	50	60	42.5
Exposed area, m² (ft²)	0.269 (2.90)	0.019 (0.206)[a]	0.022 (0.235)[a]

Wing to centerline ref. area: 0.419 m² (4.51 ft²)
Total planform ref. area: 0.573 m² (6.17 ft²)
Body length: 1.52 m (59.84 in.)

[a]One panel.

4

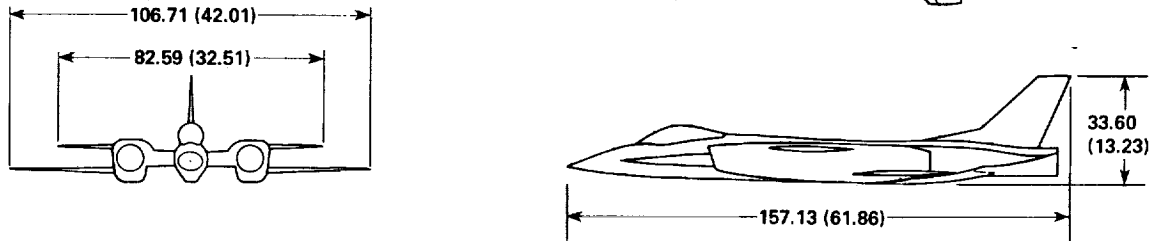EJECTOR

106.71 (42.01)
82.59 (32.51)
33.60 (13.23)
157.13 (61.86)

Fig. 4 General Dynamics Ejector configuration.

Table 3 Geometry of Ejector configuration

Property	Wing	Horizontal canard (midposition)	Vertical tail
Airfoil			
Root	NACA 64A204	NACA 64A005	5.3% biconvex
Tip	NACA 64A204	NACA 64A003	4.0% biconvex
MAC, m (in.)	0.340 (13.40)	0.183 (7.20)	0.184 (7.26)
Aspect ratio	3.62	1.08[a]	1.27
Taper ratio	0.190	0.37	0.43
Root chord, m (in.)	0.495 (19.51)	0.249 (9.82)	0.245 (9.64)
Tip chord, m (in.)	0.094 (3.71)	0.092 (3.63)	0.105 (4.14)
Span, m (in.)	1.067 (42.01)	0.184 (7.26)[a]	0.222 (8.75)
Dihedral, deg	0	0	---
Incidence, deg	0	---	---
Twist (positive LE up at tip), deg	0	0	0
Hinge line			
B.L., m (in.)	---	0.228 (9.00)	0
F.S., m (in.) (coincident with 0.25 MAC)	---	0.620 (24.41)	1.252 (49.30)
W.L., m (in.)	---	0.396 (15.59)	0.403 (15.87)
Hinge-line sweep, deg	---	1.8	0
Leading-edge sweep, deg	40	45	47.5
Exposed area, m² (ft²)	0.128 (1.374)	0.029 (0.308)[a]	0.039 (0.419)

Wing to centerline ref. area: 0.315 m² (3.39 ft²)
Total planform ref. area: 0.671 m² (7.22 ft²)
Body length: 153 m (60.10 in.)

[a]One panel.

lift comes from the wing. A problem arises, however, with the subject models in that much of the lift is generated by components other than the wing. The lift-enhancing surfaces of each model account for different percentages of the total lift, and their areas are not accounted for in the "usual" lift coefficients. This can lead to difficulty in interpreting the aerodynamic characteristics of the models, as illustrated in the left-hand plot of Fig. 5. For example, without consideration of the reference areas, it would appear that the Ejector model generates far more lift at all angles of attack than the other models. This is not necessarily true, however, because of the different relative sizes of the primary lifting surface on each model. A new reference area will be defined to reduce this misinterpretation.

Since the secondary lifting surfaces are so significant on these models, it is appropriate to consider their area when comparing lift and drag coefficients. However, it is difficult to define the boundaries between the fuselage and both primary and secondary lifting surfaces. In addition the fuselages and nacelles contribute significantly to the lift. Therefore, the reference area selected here is the total planform area. The effect of this (Fig. 5, right side), is a large reduction in lift-curve slope for the Ejector model, which had the relatively small original reference area, and lesser, yet significant, reductions in lift-curve slope for the other models. All the data presented in this paper, with the exception of Fig. 10, will use total planform areas as the reference areas.

Analysis of Lift-Enhancing Surfaces

Two types of effects are considered here: 1) effects caused by differences in planform shape of the lift-enhancing surfaces, and 2) effects caused by differences in position of the lift-

enhancing surfaces relative to the wings. The VATOL and RALS configurations, because of their different types of lift-enhancing surfaces (i.e., LEX and canard), are used to show the planform effects as the first part of the analysis (Figs. 6 to 10). The position effects are illustrated by plots of the RALS and Ejector configurations, since they both use canards as the lift-enhancers for the wings but in different positions relative to the wings (Figs. 11 to 15).

Planform Effects

The shapes of the lift-enhancing surfaces considered in this part of the analysis are highlighted in Fig. 6. The VATOL LEX has a curved planform extending from the wing leading edge at about 15% of the exposed wing semispan to the fuselage at a point about halfway between the nose and the wing-fuselage juncture. The ratio of exposed LEX planform area to the reference area used in this paper (i.e., total model planform area) is 4.9%. The complex curvature of the LEX can be seen in the front view, which gives an indication of its varying thickness and of its camber and twist. The canard on the RALS model has an exposed semispan of 36% of that of the wing, and its exposed area is 6.6% of the model reference area. The canard is separated from the wing by a small longitudinal gap and a difference of 8° in dihedral angles. (The wing of each of these two models is actually the same piece of hardware.)

The planform effects of the lift-enhancing surfaces of these two models are discussed in the following subsections.

LEX and Canard On/Off Effects. Effects of having the LEX and the canard either on or off are shown in Fig. 7. Data are presented in terms of lift, drag, and lift-to-drag ratios for Mach numbers of 0.6, 0.9, and 1.2.

BASELINE CONFIGURATIONS M = 0.6

ORIGINAL REFERENCE AREA: WING TO FUS. c_L

REVISED REFERENCE AREA: TOTAL PLANFORM AREA

	REFERENCE AREA, ft^2
△ VATOL	4.51
□ RALS	4.51
○ EJECTOR	3.39

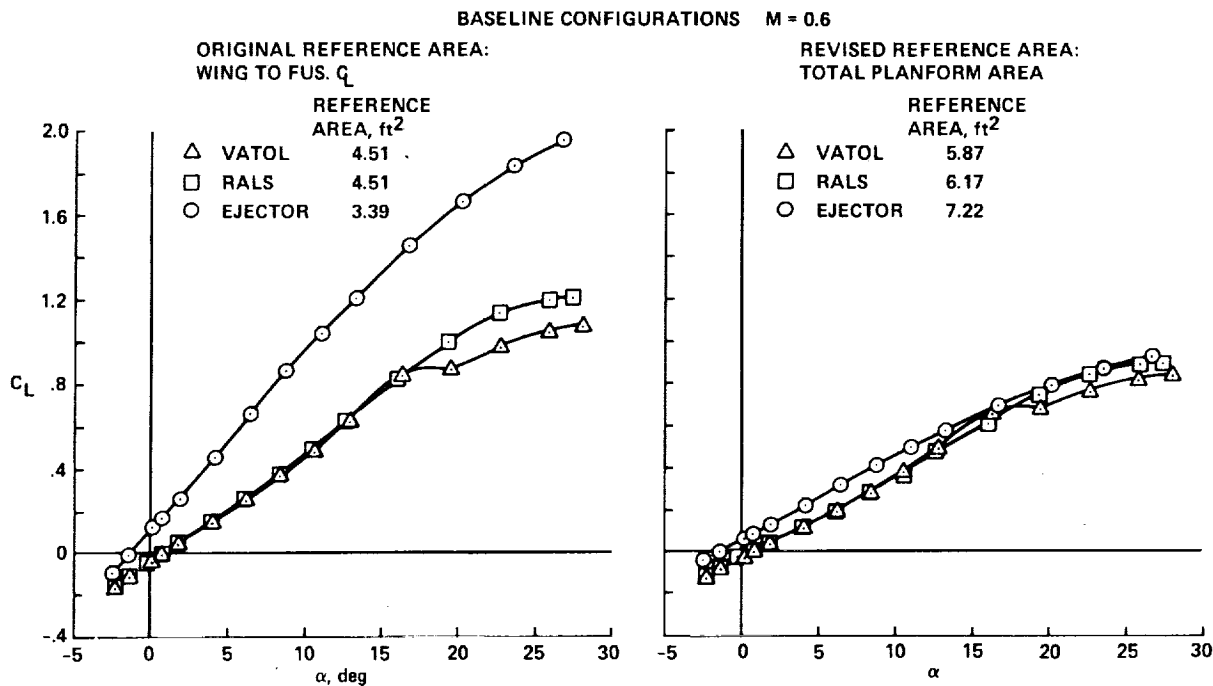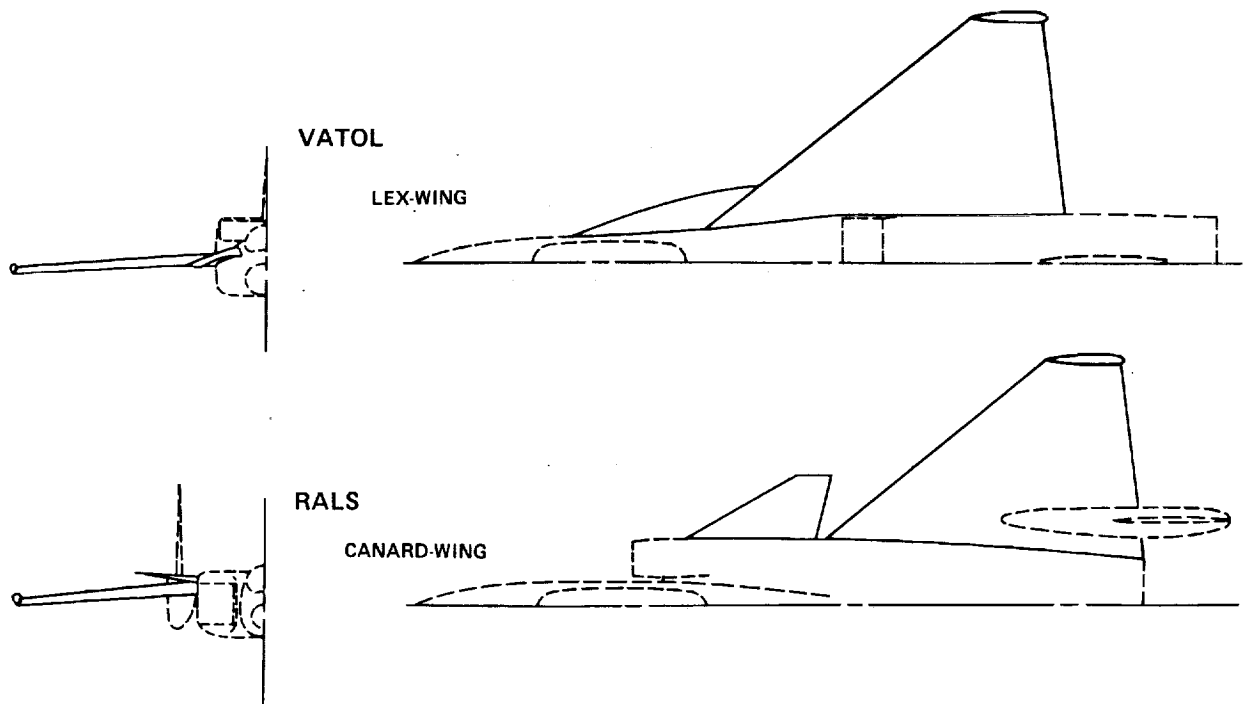|	REFERENCE AREA, ft^2
△ VATOL	5.87
□ RALS	6.17
○ EJECTOR	7.22

Fig. 5 Reference area comparisons.

Fig. 6 Planform effects: LEX-wing and canard-wing configurations.

Installing the LEX on the VATOL model improves the wing flow. At angles of attack below 10°, the LEX has essentially no effect on the overall lift and causes only a very slight increase in drag, resulting in reduced maximum lift-to-drag ratios relative to the LEX-off cases. Above this angle, and for speeds other than supersonic, the LEX increases the slope of the lift curve and causes a substantial reduction in drag. Supersonically, addition of the LEX does not significantly affect the lift or drag at the higher angles of attack.

With the lift-enhancing surfaces on, there is a notable difference between the VATOL and RALS configurations. This difference is the break in the VATOL subsonic lift and drag curves at angles of attack of about 16° to 23°, contrasted to the smoothness of the RALS curves up to the maximum angles. This break in the VATOL curves results in a leveling off or slight reduction in lift at an angle of attack of about 16° and an increase in drag. The result is a sharp reduction in L/D in this region of maneuver lift coefficients (C_L). As the Mach number is increased, the lift coefficient at which the break occurs increases also. For example, at M = 0.6, $C_L \approx 0.7$ at the break. It moves up to 0.8 at M = 0.9. At M = 1.2, the break does not occur up to the highest lift coefficient attained $(C_L = 1.0)$. This trend of increasing lift coefficient at the break with increasing Mach number indicates that the beneficial vortex interaction with the wing is being retained to higher angles of attack at higher speeds.

The canard of the RALS model produces similar or even more benefits than the LEX of the VATOL model. These benefits do not degrade with initial "breaks" at the higher angles of attack as with the LEX. The canard-on data show benefits from angles of attack as low as 5°. The lift and drag improvements caused by adding the canard at subsonic speeds result in higher lift-to-drag ratios at the higher

lift coefficients, but not in the region of maximum L/D. At supersonic speeds there is a significant reduction in overall L/D at all C_L's.

The relative effectiveness of the lift-enhancing surfaces is influenced by the difference in the bodies of the two configurations. The shape of the forebody and the placement of the wing on the body affect the flow over the wing. Also, the cross-sectional shape of the body itself can have a substantial effect on the overall aerodynamic characteristics. The dashed curves in Fig. 7 reveal what are basically the wing-body characteristics of the VATOL and RALS configurations. Generally, the VATOL wing-body generates more lift and less drag than that of the RALS, up to an angle of attack of about 18°. Above 18°, the lift of the VATOL increases more slowly compared with that of the RALS. This wing-body characteristic of the VATOL contributes to the aforementioned "break" in the LEX-on aerodynamics. These differences in the wing-body characteristics influence the relative benefits of the lift-enhancing surfaces, and must be considered when the merits of these surfaces are assessed.

The incremental benefits of a lift-enhancing surface can be demonstrated by a parameter that shows the additional or synergistic lift increase that results from this added surface. This parameter, f_L, is termed the "lift-enhancing surface lift efficiency factor," and is defined as

$$f_L = \frac{C_{L_{TOT}}}{C_{L_{(-a)}}} \cdot \frac{S_{REF} - S_a}{S_{REF}}$$

where $C_{L_{TOT}}$ is the total lift coefficient of the configuration with the additional surface (i.e., LEX or canard); $C_{L_{(-a)}}$ is the lift coefficient
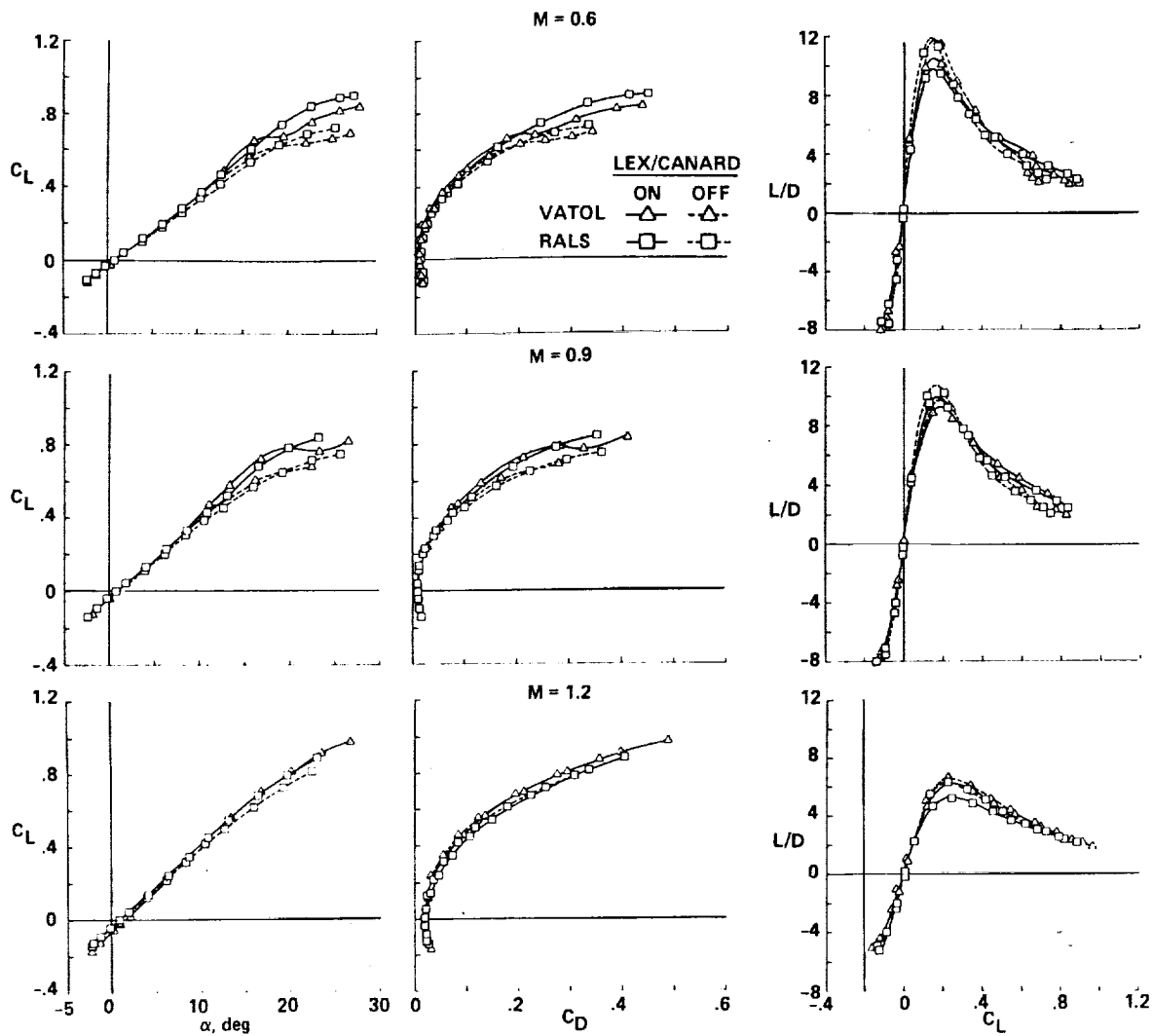
7

Fig. 7 Basic lift and drag characteristics: VATOL and RALS models.

without the additional surface; S_a is the exposed planform area of the additional surface; and S_{REF} is the model reference area (defined here as the total planform area, which includes S_a, even when the additional surface is off). A similar factor, f_D, is defined for drag, which uses drag coefficients in place of the lift coefficients in the above definition. Note that in contrast to the lift factor, a low drag factor is better than a high one. These two factors are plotted in Fig. 8 from the data presented in Fig. 7. Data for an alternate LEX (Fig. 2), having one half the planform area of and the same shape as the standard LEX on the VATOL configuration, is also plotted (discussed in next section).

The purpose of this efficiency factor is to show when a lift-enhancing surface provides a lift increase in excess of that expected from an increase in planform area of the original shape. For example, when the lift factor equals 1, the increase in lift due to the additional surface is exactly in proportion to the increase in area. In this case, the addition of the surface does no more than would adding an equivalent amount of wing area.

Several aerodynamic characteristics previously mentioned are highlighted by the efficiency factor curves (Fig. 8). The break in the lift curve at M = 0.6 of the VATOL (standard) LEX (Fig. 7) shows up as a distinct dip in the corresponding f_L curve at the same angle of attack — about 16°. The lift efficiency recovers above $\alpha = 20°$, where improvements caused by the LEX of $f_L = 1.15$ are shown. In the drag factor curve (lower part of Fig. 8) at M = 0.6, one must not confuse the peak at $C_L = 0.2$ with the dip in the f_L curve. The peak at this low C_L illustrates the drag penalty of the LEX at angles of attack less than 5°. The aforementioned lift curve break at $\alpha = 16°$ corresponds to the downward plunge of the f_D curve at $C_L = 0.6$. (Note the increasing difference between the LEX-on and LEX-off drag curves starting at about $C_L = 0.6$ at M = 0.6 in Fig. 7.) The f_L curve for the VATOL at M = 0.9 shows lift increases similar to those at M = 0.6, except that the dip occurs at $\alpha = 20°$ instead of 16°. Beyond this angle, the lift benefits are lower at M = 0.9 than at M = 0.6. The drag benefit at M = 0.9 is very evident in the lift coefficient range of the relatively high lift efficiency factors ($C_L = 0.4$ to 0.8). At M = 1.2, the LEX produces no positive

8

$$f_{L,D} = \frac{C_{L,D_{TOT}}}{C_{L,D_{(-a)}}} \cdot \frac{S_{REF} - S_a}{S_{REF}}$$
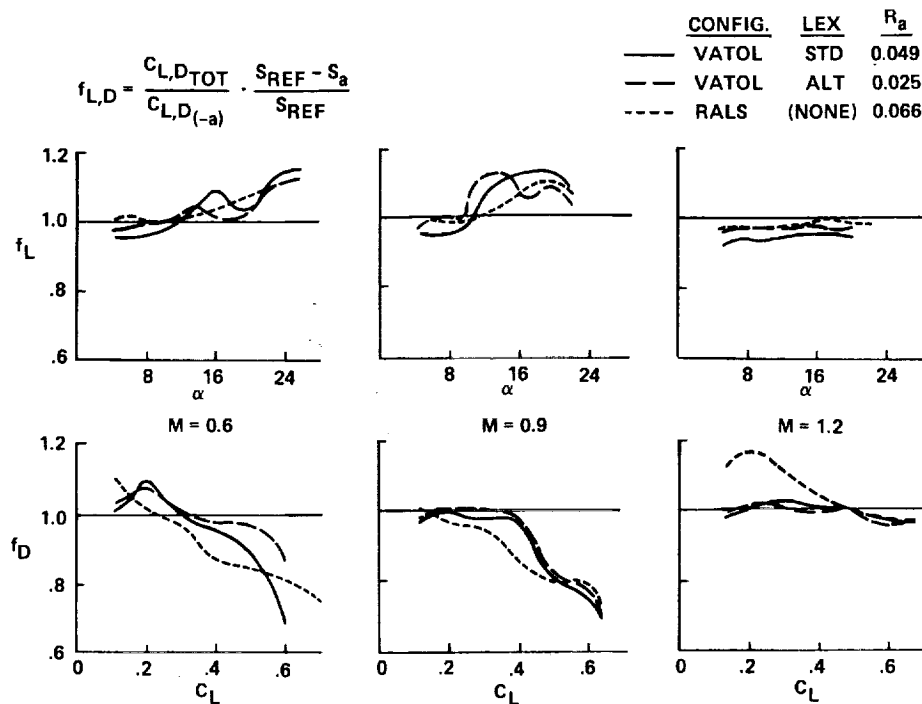
Fig. 8 Lift-enhancing surface efficiency factors: VATOL and RALS models.

lift interference and a slight drag penalty over the entire lift coefficient range.

The efficiency factors for the RALS configuration (Fig. 8, short-dashed curves) show that at subsonic speeds, addition of the canard yields increasing lift and drag benefits with angle of attack. Positive lift interference occurs above $\alpha = 10°$ for both M = 0.6 and 0.9, and increases in lift of slightly over 10% are shown at the maximum angles before stall. More significant improvements from the canard are seen in the drag factors, where drag is reduced by about 25% at the highest lift coefficients for subsonic speeds. However, at M = 1.2, the canard has a substantial drag penalty at the lower lift coefficients. Over the range of angles tested at this speed, the lift factor never exceeds 1, and the drag factor shows nearly a 20% increase in drag at about $C_L = 0.2$. For this configuration the canard-wing interference is detrimental to the overall lift and drag at M = 1.2.

LEX Size Effects. The large dashes in Fig. 8 represent the lift and drag efficiencies of the VATOL model with the smaller, alternate LEX. The efficiencies of the smaller LEX exhibit characteristics similar to those of the larger (standard) LEX, except of generally lower magnitudes. There is a peak in the M = 0.6 lift efficiency curve at $\alpha \cong 14°$ for this half-size LEX, but both the angle at which the peak occurs and the magnitude of the peak are lower than those of the standard LEX. The drag benefit is lower at this Mach number, as indicated by the higher values of f_D at the upper lift-coefficient range. Increasing the Mach number to 0.9 reduces the lift factor for the alternate LEX at the higher angles (above approximately $\alpha = 14°$). At M = 1.2, the lift benefits of this smaller LEX disappear, as they did for the larger LEX. The drag factors at these two higher Mach numbers are the same as those of the larger LEX.

Curves of C_L and C_D in Fig. 9 help explain the shapes of these efficiency factor curves. Results are shown for the standard and alternate LEX's and LEX-off. With the alternate LEX, the model generates lift equal to that of the standard LEX up to angles of attack of 13° to 15°, after which the lift is less for the alternate LEX. The lift curve for this smaller LEX at M = 0.6 does not break and recover, however, as it does for the standard LEX; the lift degrades smoothly up to the stall angle. The peak in the corresponding efficiency curve for the alternate LEX is caused by the LEX-off lift paralleling the alternative LEX lift in the region of the peak (at about $\alpha = 13°$). (Since f_L is a ratio of lifts, two curves of the same slope yield decreasing efficiency factors.) At $\alpha = 20°$, the lift of the two LEX's is the same, yielding similar efficiencies of about 1.07. Above $\alpha = 20°$, the standard LEX has about a 5% lift advantage over the alternate LEX. At M = 0.9, a comparable advantage exists for the standard LEX at the higher angles, although the alternate LEX lift does break and recover in a way similar to that of the standard LEX.

The drag at M = 0.6 in Fig. 9 increases by as much as 20% at a lift coefficient of about 0.65, when the size of the LEX is decreased from the standard to the alternate sizes. At M = 0.9, drag increases (up to 45%) caused by decreasing LEX size are shown, depending on the lift coefficient. (Data are not presented for M = 1.2 because the lift and drag are identical for the two LEX sizes.)

These substantial lift and drag advantages of the larger LEX clearly indicate that better performance is achieved by increasing the size of the lift-enhancing surface. One contributor to this better performance is believed to be the longer length achieved by the vortex from the larger LEX before bursting. Parametric studies of LEX-wing
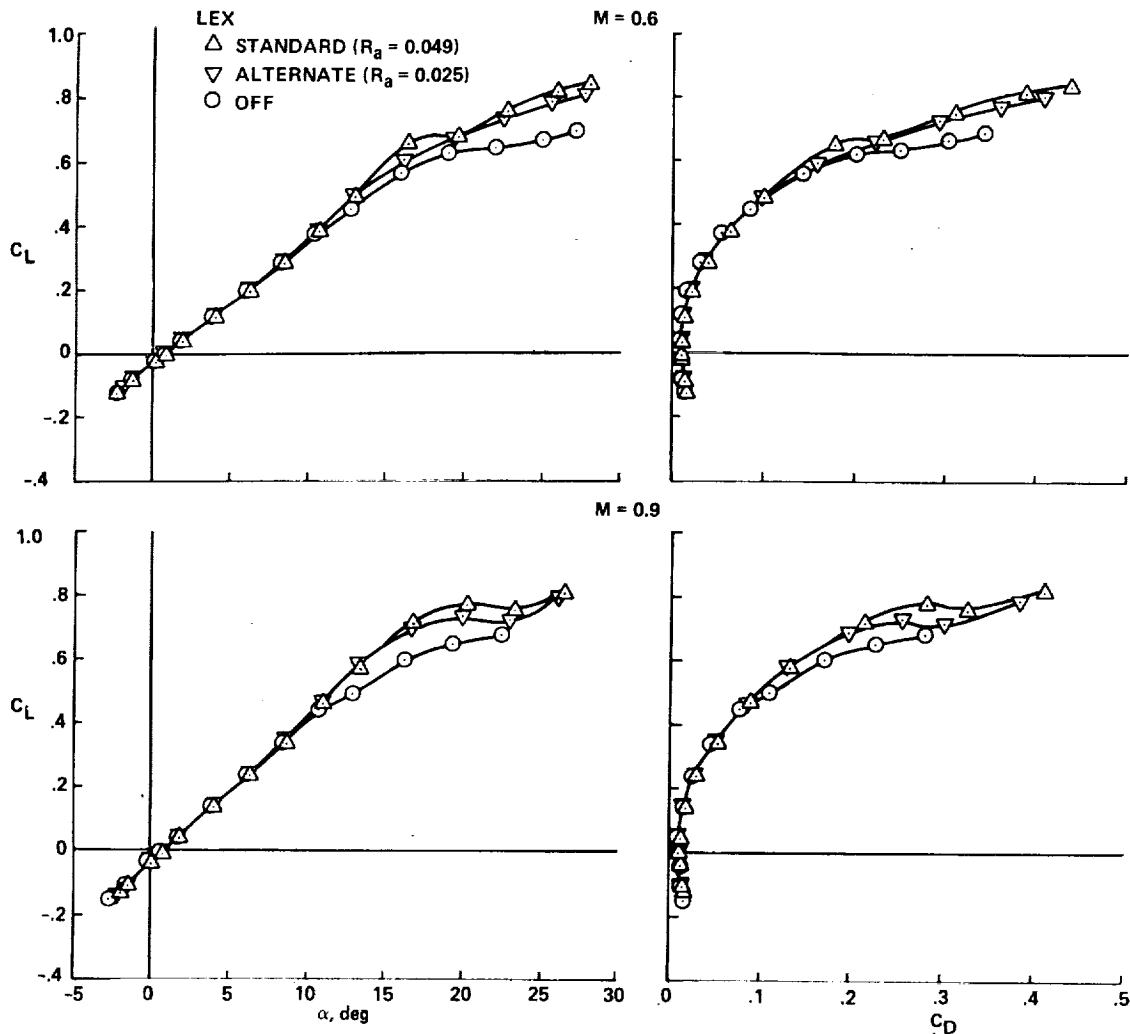
Fig. 9 Effect of LEX size on VATOL model.

configurations by Moore et al.[14] demonstrate how the vortex burst point moves aft with increasing LEX size at a given angle of attack (Figs. 17 and 18 in Ref. 14).

Figure 10 is a different version of the f_L plot at M = 0.6 shown in Fig. 8. It also includes data from tests at Langley Research Center by Luckring[12] of various LEX and canard configurations. Note that the reference areas used to generate these curves are the wing planform areas extended to the fuselage centerlines, instead of the total planform areas, as used elsewhere in the present paper. The R_a values were calculated here using the wing area extended to the centerline for all configurations.

The model of Ref. 12 is generic in nature, having the capability of testing various size LEX's and canards with the wing. The fuselage is essentially a body of revolution with the wing mounted along the centerline. The LEX mounts in the plane of the wing, and the canard mounts above the plane of the wing. The tests in Ref. 12 were conducted at M = 0.3.

Luckring's data suggest that lift efficiency increases with increasing size of either the LEX or canard relative to the wing size. The VATOL LEX's with R_a = 0.032 or 0.064 show efficiencies

approximately the same as the generic model with the smallest LEX (R_a = 0.08). The generic model with a LEX with R_a = 0.27 shows efficiencies of over 1.3 before reaching the maximum angle of attack. Similarly, the best efficiency of the RALS canard (R_a = 0.092) is about 1.1 at maximum angle of attack; the larger generic model canard (R_a = 0.28) reaches an f_L of 1.25. As with the LEX's, increasing the size of the canard produces greater lift efficiencies. An extension of this trend to the VATOL and RALS models suggests that increasing the respective LEX and canard sizes would yield significantly higher efficiencies. However, the primary advantage of a LEX or canard is in maneuvering flight, and this must be balanced by the possible disadvantages of increasing the size of these surfaces, such as decreased longitudinal stability, increased cruise drag, and possibly detrimental lateral/directional effects.

Position Effects

This part of the analysis focuses on the two canard configurations since none of the LEX shapes was tested in different positions. The relative positions of the canards and wings on the two configurations are shown in Fig. 11. On both, the canard and wing are closely spaced longitudinally,

10

REFERENCE AREA = S_{WING} TO $\mathcal{L}$
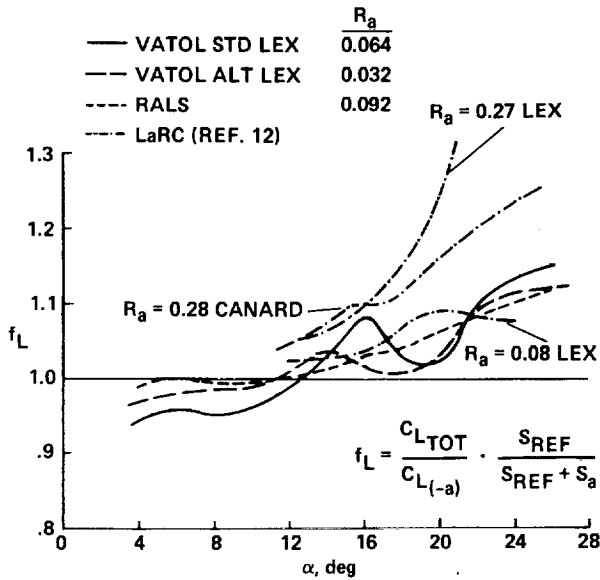
M = 0.6 (EXCEPT REF. 12 IS M = 0.3)

	R_a
—— VATOL STD LEX	0.064
— — VATOL ALT LEX	0.032
---- RALS	0.092
—·— LaRC (REF. 12)	

$R_a = 0.27$ LEX

$R_a = 0.28$ CANARD

$R_a = 0.08$ LEX

$$f_L = \frac{C_{L_{TOT}}}{C_{L_{(-a)}}} \cdot \frac{S_{REF}}{S_{REF} + S_a}$$

Fig. 10 Lift-efficiency factors: VATOL, RALS, and Langley models.

and the primary difference in positioning is in the vertical spacing and dihedral angle. There is a vertical gap of only 5% of the wing MAC (2.64 cm) between the canard tip and wing (at the span station of the canard tip) on the RALS, and there is a difference of 8° dihedral between the two. The dihedral angles of the Ejector canard and wing are set at 0°, and their vertical gap is approximately 23% of

the wing MAC (7.72 cm). Three different longitudinal locations for the canard were tested on the Ejector model as shown in Fig. 11. The midposition is considered the baseline. The forward and aft positions are each at distances of 25% of the wing MAC (8.6 cm) from the baseline position. There is a large difference in the sizes of the canards relative to the wings on each configuration. On the RALS, the canard exposed planform area is 14% of the wing exposed planform area; on the Ejector it is 45%.

Canard On/Off Effects. Figure 12 shows the lift and drag of the RALS and Ejector models with and without the canard installed. Both models exhibit significant improvements in lift and drag due to the addition of the canard. At a Mach number of 0.6, positive lift increments are seen for both configurations from angles of attack as low as 5°. There is a large difference between the two models in the magnitudes of these increments at all angles of attack above 5°. The RALS canard shows a steadily increasing benefit up to the maximum angles of attack; that is, the canard-on and -off lift curve slopes are nearly constant up to the stall breaks. The Ejector canard lift increment does not steadily increase with angle of attack. With the canard off at M = 0.6, the Ejector lift breaks at $\alpha = 5°$ then recovers at about $\alpha = 15°$. The result is a relatively large canard-addition lift increment from the canard-off break point upward. At an angle of attack of 16°, at which the difference in the canard on/off increments between the two models is the greatest, the Ejector canard shows a lift increase of 43%; the RALS canard shows an increase of only 12%.

Two primary factors account for the differences in the canard-off lift between the two configurations. The Ejector wing has a leading-edge sweep
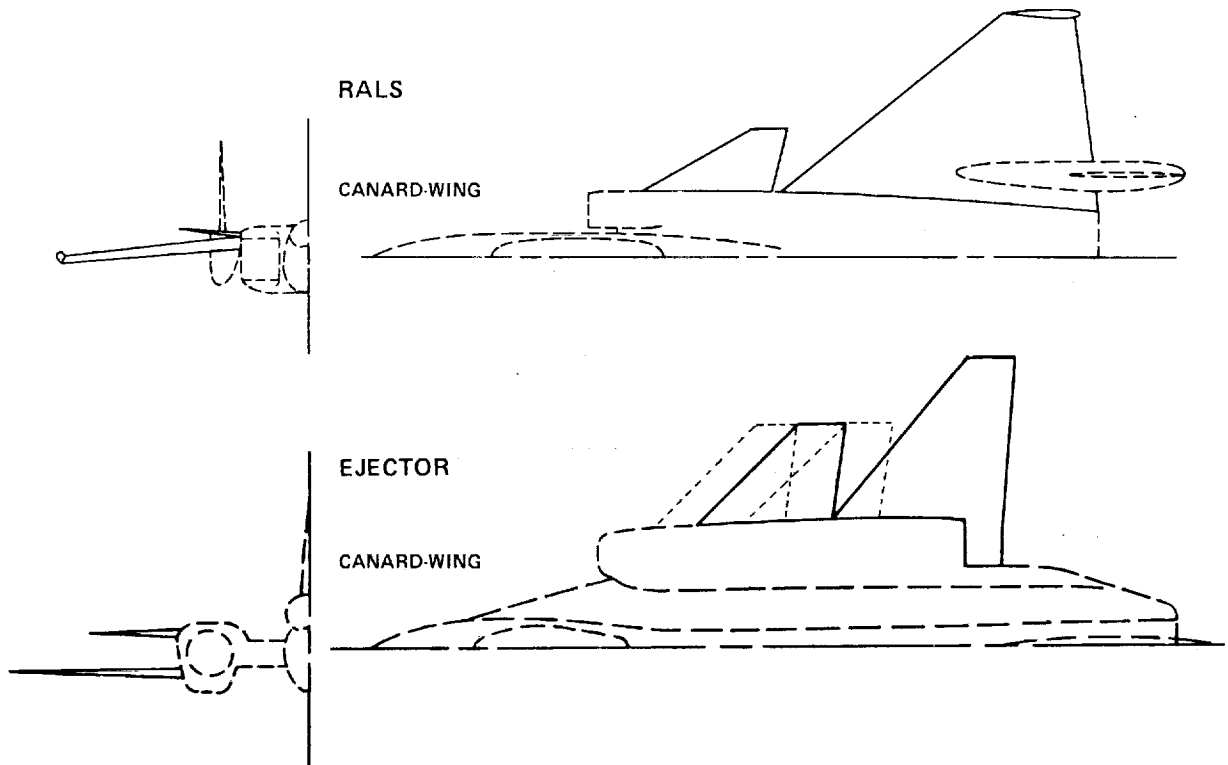
RALS

CANARD-WING

EJECTOR

CANARD-WING

Fig. 11 Position effects: two canard-wing configurations.
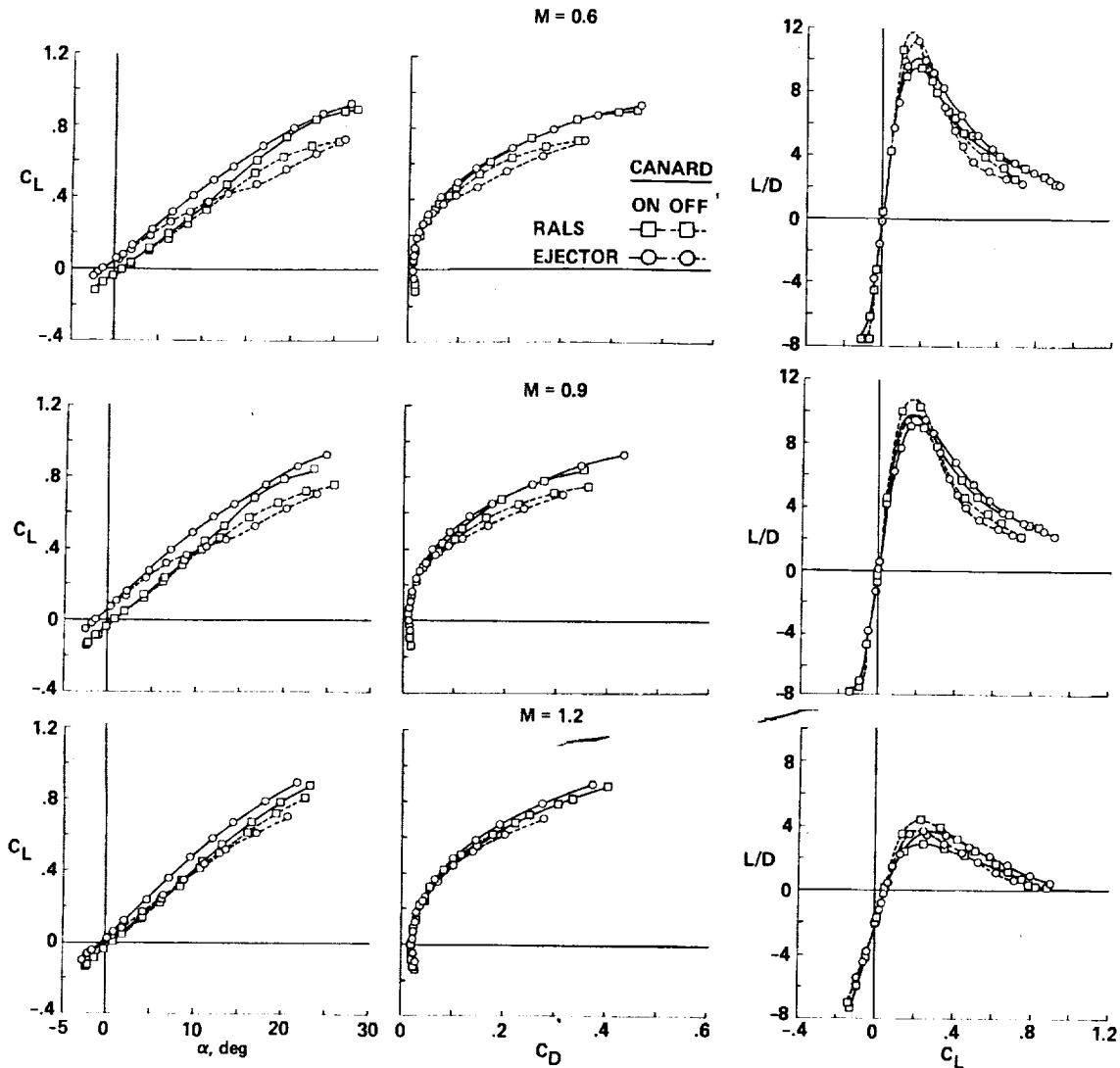
11

Fig. 12 Basic lift and drag characteristics: RALS and Ejector models.

angle (40°) that is lower than that of the RALS (50°); this results in decreased lift at the higher angles of attack. Gloss and McKinney[15] tested wings of 44° and 60° leading-edge sweep with canards removed; they found a similar decrease in lift at higher angles of attack for the wing with less sweep (44°). In addition, the RALS wing has 6° of twist and the Ejector wing has none. This delays separation on the outboard portion of the RALS wing, which contributes to its relatively good lift at high angles of attack.

The increment in total model lift caused by the canard is affected by other geometrical differences between the models. The exposed span of the RALS canard is only 32% of the wing exposed span; this span ratio on the Ejector model is 61%. Much more of the wing flow is influenced by the presence of the canard on the Ejector Model, which explains some of the larger lift improvement from the canard on this model. Also, the difference in vertical spacing between the canard and wing on each of the two models (as previously discussed) accounts for some of this increment. Data from Refs. 15 and 16, for canards tested in the wing chord plane and at 18.5% MAC above it, show that canard-wing interfer-

ence is improved slightly by moving the canard above the wing plane.

A factor that tends to increase the RALS lift increment over that of the Ejector is the higher leading-edge sweep of the RALS canard (60° for the RALS and 45° for the Ejector). Gloss[16] found that increasing the canard sweep angle increased the total configuration lift at the higher angles of attack. Although this influence of sweep never gives the RALS canard a greater lift increment than that of the Ejector canard, it tends to decrease somewhat the advantage of the Ejector canard over the RALS.

At M = 0.9, the relative magnitudes of the canard lift increments for each model in Fig. 12 are about the same as they are at M = 0.6. The magnitude of this increment is significantly reduced at M = 1.2, primarily because of the increased canard-off lift. The Ejector canard lift increment at M = 1.2 is reduced slightly from the subsonic cases. The supersonic flow improves the wing lift in the presence of the body alone and at the same time reduces the beneficial canard-wing interference effects.

12

Addition of the canard at $M = 0.6$ reduces drag by about 35% on the Ejector model and about 25% on the RALS at $C_L = 0.7$. These relative reductions are consistent with the positive lift increments at the same Mach number; that is, the RALS canard reduces drag slightly at lift coefficients in the midrange and much more at the higher coefficients. On the other hand, the Ejector canard generates a large reduction increment starting at about $C_L = 0.4$, and this increment does not increase as rapidly as that for the RALS up to the higher lift coefficients.

For both the RALS and Ejector configurations, there is little change in the drag increments due to the canard from $M = 0.6$ to 0.9. At $M = 1.2$, the drag advantage of the RALS canard becomes very small, as does the lift advantage previously discussed.

Lift-to-drag ratios at all Mach numbers show that there is a substantial penalty in maximum L/D for having the canard on both configurations. The advantage of the canard in terms of L/D is at the highest lift coefficients, where improvements of up to 50% are shown for both models at subsonic speeds. At $M = 1.2$, the RALS canard shows no L/D improvements; at the same Mach number, the Ejector canard increases L/D about 30% at the maximum C_L.

Figure 13 shows the lift and drag efficiency factors for the RALS and Ejector configurations. At the subsonic Mach numbers, the Ejector canard shows lift efficiencies of 1.2 or better at angles of attack above 12°, with reductions in drag effi-

ciency factors (f_D) to 0.6 at the higher angles. In comparison, these lift and drag improvements at subsonic speeds are about twice as large as those for the RALS, which had maximum lift efficiency factors of 1.1 and minimum drag factors of 0.8. At $M = 1.2$, the improvements are reduced slightly for the Ejector model for which lift and drag factors are limited to about 1.1 and 0.7, respectively. As previously discussed, these factors for the RALS at this speed show no lift benefit and substantial drag increases throughout most of the angle of attack range.

In Fig. 13, the lift factor for $M = 0.6$ includes data from Ref. 15 that support the postulate that a large, high-mounted canard has better interference effects than a small, low-mounted one. The specific configuration selected from Ref. 15 is a general research model that has a canard in a horizontal and vertical position similar to that of the Ejector model (the vertical spacing between the canard and wing on the research model is about 18% of the wing MAC, or 4.29 cm). The ratio of canard to total planform area (R_a) for this model is 0.098, which is 14% higher than that for the Ejector, but the exposed canard to wing span ratio (47%) is lower than that for the Ejector (61%). The interference lift on this configuration is high $(f_L > 1.2)$ above angles of attack of about 18°, as is the interference lift on the Ejector at $\alpha = 12°$ and above. As noted in the discussion of LEX size effect on interference lift, it appears that improvements on both the RALS and Ejector models can be achieved by increasing the size of the canards.

CONFIG.	CANARD POS.	R_a
RALS	(INVARIANT)	0.066
EJECTOR	FWD	0.086
EJECTOR	MID	0.086
EJECTOR	AFT	0.086

$$f_{L,D} = \frac{C_{L,D_{TOT}}}{C_{L,D_{(-a)}}} \cdot \frac{S_{REF} - S_a}{S_{REF}}$$
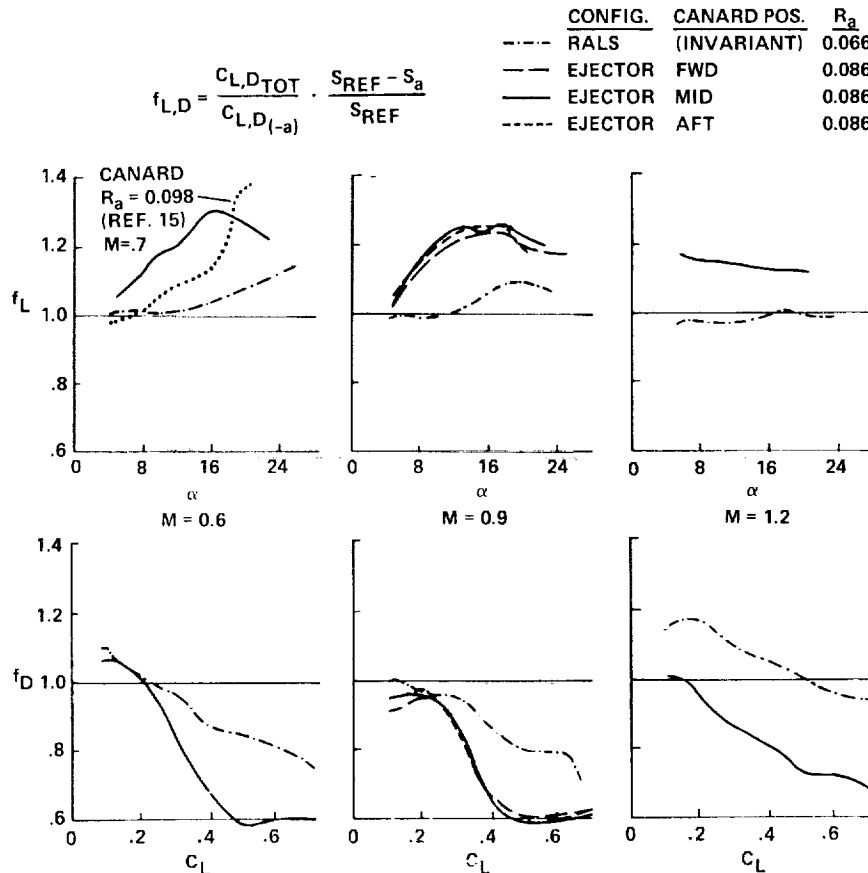

Fig. 13 Lift-enhancing surface efficiency factors: RALS and Ejector models.

Canard Location Effects. The influence of canard location on interference lift and drag is shown in the efficiency factor curves for M = 0.9 in Fig. 13. The canard at the midlongitudinal position (baseline) has about the same lift and drag factors as do the other two positions. Figure 14 presents the lift and drag coefficients of the Ejector model with the canard in the three positions. The data show a slightly higher lift and lower drag at the higher angles of attack for the midcanard position. From these two figures, it is evident that the variations of longitudinal location of the canard available on the model did not have a substantial influence on the amount of interference lift and drag on the Ejector configuration. (Data are shown only for M = 0.9 since the Mach effects on canard location are small.)

Canard Deflection Effects. Figure 15 shows the effect of deflecting the canards on the RALS and Ejector configurations. There is a general trend for both configurations of increasing lift increment for positive canard deflections with increasing angle of attack. At α = 20°, the lift increment becomes negative at the canard deflections of +10°. This decrease in lift is believed to be a result of the canard stalling at the locally high angle of attack. The drag increment increases with the increasing lift, but it reduces when the canard stalls. The favorable interaction between the canard and wing is disrupted at canard stall, and there is a decrease in overall model lift and an associated decrease in induced drag.

At the negative canard deflections, the reductions in lift at all angles of attack are the
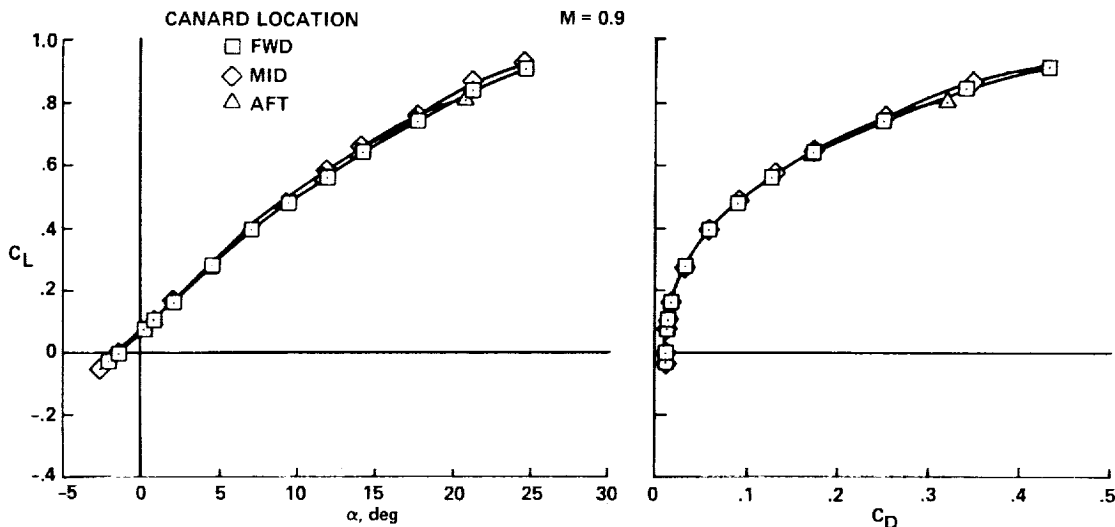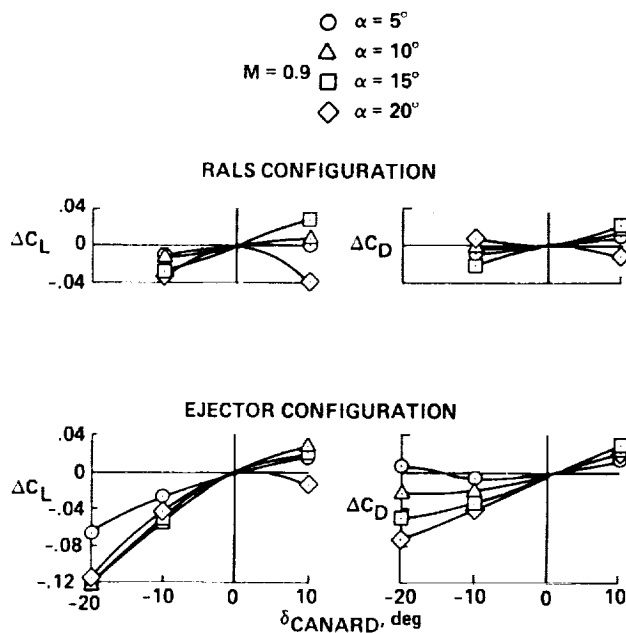

Fig. 14 Effect of canard location on Ejector model.

Fig. 15 Effect of canard deflection on RALS and Ejector models.

14

result of the negative canard lift overriding the slight increase in wing lift from the canard upwash field. These lift reductions are greater for the Ejector model compared with the RALS, probably because of the large canard span relative to the wing on the Ejector model (see Fig. 11). Likewise, the drag of the Ejector is reduced more than the drag of the RALS for negative canard deflections.

Conclusions

Forward lift-enhancing surfaces significantly improve the overall lift and drag characteristics on generic research configurations. Their effects on realistic V/STOL fighter/attack aircraft configurations have been analyzed in this paper. In particular, three V/STOL fighter configurations were considered. One of these, the "VATOL," employed a leading-edge extension (LEX) as the lift-enhancing surface, while the other two, the "RALS" and the "Ejector" configurations used all-movable canards. The basic lift and drag characteristics of the three configurations were quantified, the relative efficiencies of their lift-enhancing surfaces examined, and the effects of different LEX sizes, canard deflections, and varying canard locations were considered. The major findings of this analysis are as follows.

Planform Effects

1) At angles of attack above 10° at subsonic speeds, the LEX improved the lift (up to 15%) and the drag (up to 40%) of the VATOL model. There were no lift or drag benefits at $M = 1.2$.

2) At an angle of attack of about 16°, there was a notable break in the lift curve of the VATOL model, at which a loss of lift and an increase in drag occurred. The break was probably caused by the vortex bursting and breaking down the favorable flow interaction with the wing.

3) There were fewer benefits associated with a smaller, alternate LEX on the VATOL than with the standard LEX. Similarly, there were fewer benefits with the RALS canard than with a general research model canard with a larger area relative to the wing. These tests and those on generic research models suggest that larger LEX's and larger canards produce greater improvements in lift and drag.

4) The canard of the RALS configuration resulted in lift enhancements of about 10% and in drag reductions of 25% at subsonic Mach numbers. At supersonic speeds, the canard provided no lift improvement and imposed a drag penalty of nearly 20%.

5) The efficiencies of the VATOL LEX and the RALS canard were comparable in overall magnitudes, though the LEX had more erratic behavior.

Position Effects

1) At $M = 0.6$, the addition of the canard on the Ejector model gave large lift and drag enhancements (over 35%). Two factors are primarily responsible for the improved flow over the wing which gives these enhancements: the large size of the canard relative to the wing, and the high position of the canard relative to the wing.

2) The lift and drag improvements resulting from the Ejector canard were degraded only slightly as the Mach numbers were advanced from the subsonic to supersonic regimes, whereas the favorable influence of the RALS canard on lift disappeared and the drag was increased over most of the C_L range.

3) Changing the canard longitudinal location by 25% MAC fore and aft did not significantly affect the lift and drag of the Ejector configuration. Of the three locations tested, the midposition (with the canard root trailing edge directly above the wing root leading edge) generally had the best lift and drag characteristics.

4) Positive canard deflections on both models gave positive lift and drag increments up to canard stall. Negative deflections reduced lift and drag on both models, although more so on the Ejector because of the large canard span relative to the wing.

References

[1]Nelms, W. P., "Studies of Aerodynamic Technology for V/STOL Fighter/Attack Aircraft," AIAA Paper 78-1511, Los Angeles, Calif., 1978.

[2]Lummus, J. R., "Study of Aerodynamic Technology for VSTOL Fighter/Attack Aircraft," NASA CR-152128, 1978.

[3]Burhans, W. R. et al., "Study of Aerodynamic Technology for VSTOL Fighter/Attack Aricraft," NASA CR-152129, 1978.

[4]Brown, S. H., "Study of Aerodynamic Technology for VSTOL Fighter/Attack Aircraft — Horizontal Attitude Concept," NASA CR-152130, 1978.

[5]Gerhardt, H. A. and Chen, W. S., "Study of Aerodynamic Technology for V/STOL Fighter/Attack Aircraft — Vertical Attitude Concept," NASA CR-152131, 1978.

[6]Driggers, H. H., "Study of Aerodynamic Technology for VSTOL Fighter/Attack Aircraft," NASA CR-152132, 1978.

[7]Nelms, W. P. and Durston, D. A., "Preliminary Aerodynamic Characteristics of Several Advanced V/STOL Fighter/Attack Aircraft Concepts," SAE Paper 801178, Los Angeles, Calif., Oct. 1980.

[8]Lummus, J. R., Joyce, G. T., and O'Malley, C. D., "Analysis of Wind Tunnel Test Results for a 9.39-percent Scale Model of a V/STOL Fighter/Attack Aircraft," NASA CR-152391, Vols. 1-4, 1981.

[9]Nelms, W. P., Durston, D. A., and Lummus, J. R., "Experimental Aerodynamic Characteristics of Two V/STOL Fighter/Attack Aircraft Configurations at Mach Numbers from 0.4 to 1.4," NASA TM-81234, 1980.

[10]Nelms, W. P., Durston, D. A., and Lummus, J. R., "Experimental Aerodynamic Characteristics of Two V/STOL Fighter/Attack Aircraft Configurations at Mach Numbers from 1.6 to 2.0," NASA TM-81286, 1981.

[11]Lummus, J. R., "Aerodynamic Characteristics of a V/STOL Fighter Configuration," AIAA Paper 81-1292, Palo Alto, Calif., June 1981.

[12]Luckring, J. M., "Aerodynamics of Strake-Wing Interactions," Journal of Aircraft, Vol. 16, Nov. 1979, pp. 756-762.

[13]Re, R. J. and Capone, F. J., "Longitudinal Aerodynamic Characteristics of a Fighter Model with a Close Coupled Canard at Mach Numbers from 0.40 to 1.20," NASA TP-1206, 1978.

[14]Moore, W. A., Erickson, G. E., Lorincz, D. J., and Skow, A. M., "Effects of Forebody, Wing and Wing-Body-LEX Flowfields on High Angle of Attack Aerodynamics," SAE Paper 791082, Los Angeles, Calif., Dec. 1979.

[15]Gloss, B. B. and McKinney, L. W., "Canard-Wing Lift Interference Related to Maneuvering Aircraft at Subsonic Speeds," NASA TM X-2897, 1973.

[16]Gloss, B. B., "The Effect of Canard Leading-Edge Sweep and Dihedral Angle on the Longitudinal and Lateral Aerodynamic Characteristics of a Close-Coupled Canard-Wing Configuration," NASA TN D-7814, 1974.